Title

Design and synthesis of orexin 1 receptor-selective agonists

Author's Names

Keita Iio,[a,c,†] Kao Hashimoto,[b,c,†] Yasuyuki Nagumo,[c] Mao Amezawa,[a,c] Taisei Hasegawa,[a,c] Naoshi Yamamoto,[c] Noriki Kutsumura,[a,b,c] Katsuhiko Takeuchi,[d] Yukiko Ishikawa,[c] Masashi Yanagisawa,[c,e,f] Hiroshi Nagase,[a,c,*] and Tsuyoshi Saitoh[b,c,*]

Affiliations

[a] Graduate School of Pure and Applied Sciences, University of Tsukuba, 1-1-1 Tennodai, Tsukuba, Ibaraki-305-8571, Japan

[b] Graduate School of Comprehensive Human Sciences, University of Tsukuba, 1-1-1 Tennodai, Tsukuba, Ibaraki 305-8575, Japan

[c] International Institute for Integrative Sleep Medicine (WPI-IIIS), University of Tsukuba, 1-1-1 Tennodai, Tsukuba, Ibaraki 305-8575, Japan

[d] National Institute of Advanced Industrial Science and Technology (AIST), Tsukuba Central 5, 1-1-1 Higashi, Tsukuba 305-8565, Ibaraki, Japan

[e] R&D Center for Frontiers of Mirai in Policy and Technology (F-MIRAI), University of Tsukuba, 1-1-1 Tennodai, Tsukuba, Ibaraki, 305-8575, Japan

[f] Department of Molecular Genetics, University of Texas Southwestern Medical Center, Dallas, TX75390, US

Abstract

Orexins are a family of neuropeptides that regulate various physiological events such as sleep/wakefulness as well as emotional and feeding behavior, and that act on two G-protein-coupled receptors, i.e., the orexin 1 (OX_1R) and orexin 2 receptors (OX_2R). Since the discovery that dysfunction of the orexin/OX_2R system causes the sleep disorder narcolepsy, several OX_2R-selective and $OX_{1/2}R$ dual agonists have been disclosed. However, an OX_1R-selective agonist has not yet been reported, despite the importance of the biological function of OX_1R. Herein, we report the discovery of a potent OX_1R-selective agonist, (*R*,*E*)-3-(4-methoxy-3-(*N*-(8-(2-(3-methoxyphenyl)-*N*-methylacetamido)-5,6,7,8-tetrahydronaphthalen-2-yl)sulfamoyl)phenyl)-*N*-(pyridin-4-yl)acrylamide ((*R*)-YNT-3708; EC_{50} = 7.48 nM for OX_1R; OX_2R/OX_1R EC_{50} ratio = 22.5). Unlike the OX_2R-selective agonist, the OX_1R-selective agonist (*R*)-YNT-3708 exhibited antinociceptive and reinforcing effects in mice more potently than the dual agonist.

Introduction

The orexin/orexin receptor system plays a fundamental role in the central nervous system and contributes to functions such as arousal and emotion. Orexin A and B (OXA and OXB, also called hypocretin 1 and 2) are hypothalamic neuropeptides derived from prepro-orexin that are specifically produced by neurons in the lateral hypothalamic area and that act on two G protein-coupled receptors, OX_1R and OX_2R.[1,2] The affinity of these peptides toward OXRs is different; OXA has a comparable affinity toward OX_1R and OX_2R, while OXB shows selectivity toward OX_2R.[1] Moreover, given that the expression patterns of OX_1R and OX_2R differ significantly, each receptor subtype has been postulated to have distinct functions under physiological conditions.[1,3,4] The orexin/OX_2R system is mainly involved in the regulation and stability of sleep and wakefulness, and its dysfunction causes the sleep disorder narcolepsy, which is characterized by excessive daytime sleepiness, cataplexy, hypnagogic/hypnopompic hallucinations, sleep paralysis, and disturbed nighttime sleep.[5–9] Accordingly, OX_2R agonists are attracting attention as potential therapeutic agents for narcolepsy.[5–8] In contrast, although dysfunction of the orexin/OX_1R system has not been implicated in the development of narcolepsy symptoms, several genetic and pharmacological studies

have revealed that the orexin/OX_1R system is involved in the regulation of sleep–wakefulness,[8,10,11] feeding behavior,[1,12] reward seeking,[4,13,14] analgesia,[15–17] energy homeostasis,[18,19] emotion,[20–23] and the autonomic nervous system.[24,25] Despite the importance of the physiological roles of OX_1R, its contribution to disease pathogenesis is not fully understood yet.

The medicinal chemistry of orexin receptor agonists has been vigorously investigated with a focus on narcolepsy therapeutics. The first potent nonpeptidic OX_2R-selective agonist, YNT-185, was discovered via a high-throughput screening and subsequent optimization, and ameliorated narcolepsy symptoms in animal models (Figure 1).[26,27] Since this report, several more OX_2R-selective small-molecule agonists have been reported,[28,29] including TAK-925, which has entered clinical trials for the treatment of hypersomnia including narcolepsy.[30] Recently, a dual orexin receptor agonist, RTOXA-43, in which the dimethylcarbamoyl group of YNT-185 was replaced with a 4-pyridyl carbamoyl group, has been disclosed to exhibit comparable agonist activity for both OX_1R and OX_2R (EC_{50} = 24 nM for both receptors).[31] Moreover, we have independently reported (*R*)-**2**, which is derived from a naphthalene-type OX_2R agonist and exhibits highly potent agonist activity for both receptors (EC_{50} = 13.5 nM for OX_1R, 0.579 nM for OX_2R).[32,33] Despite the significant progress in the development of OX_2R-selective and dual $OX_{1/2}R$ agonists, no OX_1R-selective agonists have been reported so far.

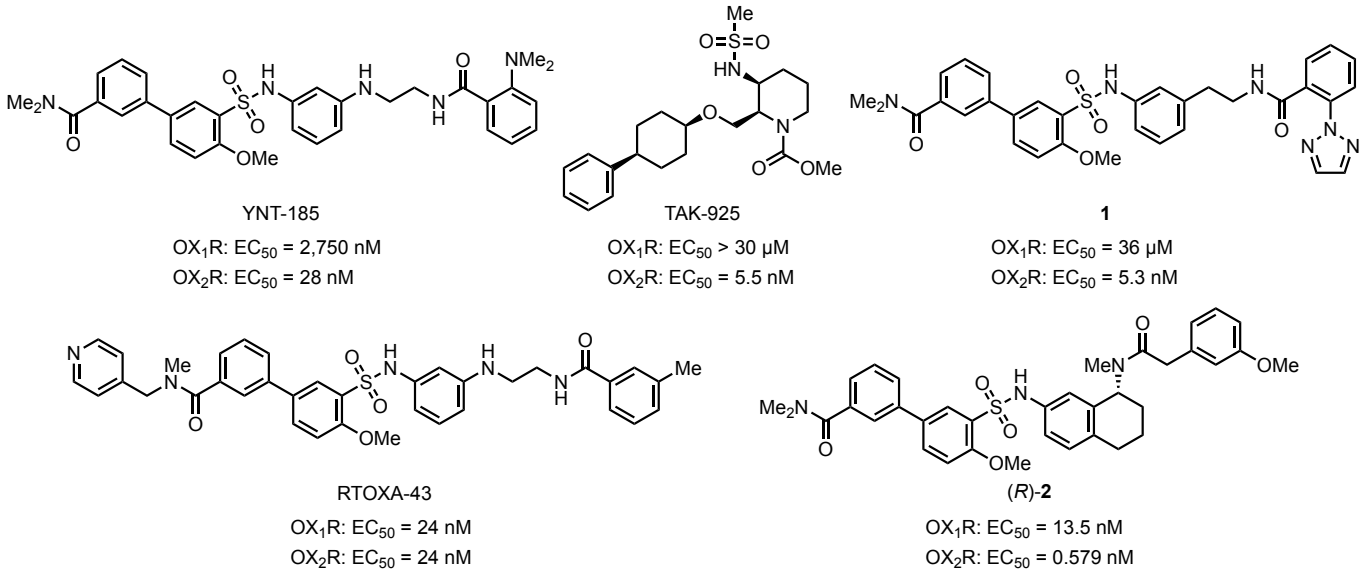

Figure 1. Structures of typical small-molecule orexin receptor agonists.

During our efforts to develop orexin receptor agonists based on the structure of (*R*)-**2**, we found that the potency of agonist activity for OX_1R and OX_2R was reversed by modification of the biphenyl sulfonamide moiety of (*R*)-**2** and discovered the first OX_1R-selective agonist, (*R*,*E*)-3-(4-methoxy-3-(*N*-(8-(2-(3-methoxyphenyl)-*N*-methylacetamido)-5,6,7,8-tetrahydronaphthalen-2-yl)sulfamoyl)phenyl)-*N*-(pyridin-4-yl)acrylamide ((*R*)-YNT-3708; (*R*)-**18**). We herein describe the process of finding (*R*)-**18** and report its *in vivo* pharmacological activity, with a focus on OX_1R-related functions such as reinforcing and analgesic effects.

In Vitro Pharmacology and Structure–Activity Relationship Studies

The structure–activity relationships of compounds obtained by modifying the biphenyl sulfonamide moiety of **2** are shown in Table 1. The removal of the dimethylcarbamoyl group on the A ring (**3**) dramatically attenuated the agonist activity against both receptors, while the removal of the A ring along with the dimethylcarbamoyl group (**4**) resulted in weak but OX_1R-selective agonist activity over OX_2R. Additionally, the removal of both the A and B rings (**5**) caused the compound to have no activity. These data suggest that the dimethylcarbamoyl group is important for potent activity, while the A ring is not essential for agonist activity, especially toward OX_1R. Encouraged by these results, we then investigated the spacer structure between the B ring and carbamoyl group to improve the activity toward OX_1R. The introduction of a dimethylcarbamoyl group directly onto the B ring improved the potency for both receptors, and **6** showed rather selective OX_2R-agonist activity. Elongation of the spacer carbon chain attenuated the activity toward both receptors (**7**–**9**), albeit that the receptor selectivity was inverted when two carbon atoms were inserted, with **8** showing a 15-fold increase in selectivity toward OX_1R compared to that of **6**. Further extension of the carbon chain improved the potency toward both receptors (**9**), while the receptor selectivity toward OX_1R decreased. Finally, the restriction of the saturated carbon chain of **8** with a double bond (**10**) further improved both the activity and selectivity toward OX_1R. Interestingly, the OX_2R-agonist activity of **6**–**10** in Table 1 differs significantly, whereas their agonist activity toward OX_1R is similar. These results imply that the A ring in the biphenyl unit efficiently interacts with OX_2R rather than OX_1R and that the double-bond spacer would be suitable for the activation of OX_1R.

Table 1. Orexin receptor-agonist activity of sulfonamide derivatives **2**–**10**

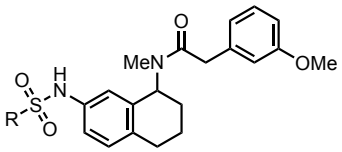

Comp.	R	EC$_{50}$ (nM) [E_{max} (%)[a]] OX$_1$R	OX$_2$R	Selectivity (OX$_2$R/OX$_1$R)
2	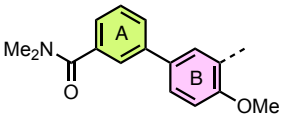	30.7 [99.6]	1.51 [104]	0.05
3	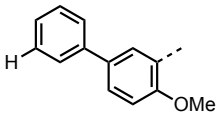	5,925 [39.0[b]]	1,289 [125]	0.22
4	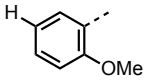	1,496 [74.1]	8,551 [67.0[b]]	5.72
5		N.A.[c]	N.A.[c]	–
6	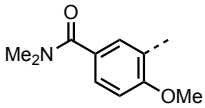	607 [95.7]	146 [121]	0.24
7	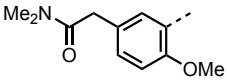	1,038 [84.3]	192 [99.8]	0.18
8	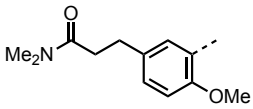	1,759 [110]	6,410 [88.1[b]]	3.64
9	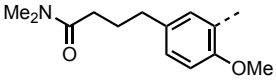	831 [125]	1,015 [114]	1.22
10	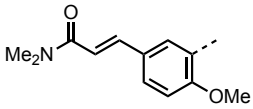	1,279 [109]	>10,000 [70.1[b]]	–

[a]E_{max} expressed as a percentage of OXA maximum. [b] Value obtained at 10 μM. [c] Not active.

As cinnamoyl derivative **10** showed moderate but selective OX$_1$R-agonist activity, we subsequently conducted a structural optimization of the substituents on the carbamoyl group, which was

assumed to be important for the potency (Table 2). Conversion of the tertiary *N*,*N*-dimethyl amide of **10** into a secondary *N*-methyl amide (**11**) or primary amide (**12**) resulted in a more than two-fold increase in agonist activity toward OX_1R, indicating that the N–H group can be expected to play an important role in the interaction with OX_1R. Although the replacement of *N*-methyl with *N*-*n*-butyl (**13**) on the secondary amide group resulted in a slight decrease in OX_1R activity, the introduction of ether oxygen and *N*-methyl nitrogen atoms increased the activity (**14** and **15**). These results suggest that the receptor pocket has enough space around the carbamoyl group and that the presence of a hydrogen-bond acceptor (HBA) on the amide sidechain is favorable for the enhancement of OX_1R-agonist activity. In order to investigate the orientation of the HBA on the carbamoyl group, we attempted to fix the basic nitrogen atom via ring formation. The 3-pyridyl derivative **16**, in which the nitrogen atom is tethered at the same distance as that of **15**, showed 6-fold more potent OX_1R-agonist activity than **15**. While moving the nitrogen atom from the 3- to the 2-position (**17**) resulted in a *ca*. 5-fold decrease in the OX_1R-agonist activity compared to that of **16**, 4-pyridyl derivative YNT-3708 (**18**) showed a significant increase in OX_1R-agonist activity and receptor selectivity. On the other hand, *N*-methyl 4-pyridyl amide **19** exhibited a 12 times weaker OX_1R-agonist activity than **18**. Moreover, anilide **20**, which does not contain HBA on the aromatic ring, showed 30 times weaker activity than **18**, which is the same activity range as *N*-methyl amide **11**. These results indicate that a suitable orientation of HBA on the *trans*-amide substituent is crucial for potent OX_1R-agonist activity.

Table 2. Orexin receptor-agonist activity of cinnamamide derivatives **10**–**20**

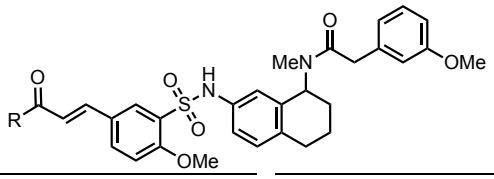

Comp.	R	EC_{50} (nM) [E_{max} (%)[a]]		Selectivity (OX_1R/OX_2R)	Comp.	R	EC_{50} (nM) [E_{max} (%)[a]]		Selectivity (OX_1R/OX_2R)
		OX_1R	OX_2R				OX_1R	OX_2R	
10		1,279 [109]	>10,000 [70.1[b]]	–	**16**	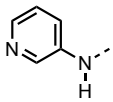	43.4 [152]	295 [130]	6.80
11	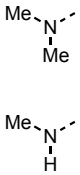	501 [99.5]	>10,000 [48.5[b]]	–	**17**	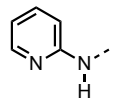	201 [81.8]	955 [101]	4.75
12		581 [95.0]	7,010 [74.5[b]]	12.1	**18** (YNT-3708)	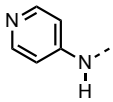	15.3 [85.4]	229 [104]	15.0

13	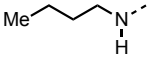	573 [98.5]	>10,000 [24.0[b]]	–	**19**	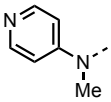	187 [110]	275 [115]	1.47
14	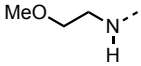	476 [116]	>10,000 [60.5[b]]	–	**20**	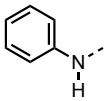	472 [97.0]	3,290 [41.3[b]]	6.97
15	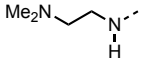	271 [151]	2,411 [92.0]	8.90					

[a] E_{max} expressed as a percentage of OXA maximum. [b] Value obtained at 10 μM.

Synthetic Chemistry and Eutomer Determination

The synthesis of the evaluated compounds is summarized in Scheme 1. The common intermediate **21** was prepared according to a previously reported method.[33] Initially, **21** was treated with 5-bromo-2-methoxybenzenesulfonyl chloride to yield intermediate **22**. Suzuki–Miyaura coupling with phenylboronic acid and hydrogenation of **22** furnished **3** and **4**, respectively. Condensation of **21** with methanesulfonylchloride afforded **5**, while **6** was obtained from a Pd-catalyzed esterification[34] followed by amidation of **23** with dimethylamine. Derivatives **7**, **9**, and **10** differ with respect to the length of their carbon chain and were synthesized using the corresponding sulfonyl chlorides (**25a**–**c**), which were prepared from the corresponding anisole derivatives (**24a**–**c**) and treated with amine **21** to provide the corresponding esters (**26a**–**c**). The latter were converted into amides **7**, **9**, and **10** *via* hydrolysis under basic conditions followed by a condensation with dimethylamine. Moreover, **8** was obtained from the hydrogenation of amide **10**. The other cinnamoyl derivatives (**11**–**20**) were synthesized in the same manner as **10**, using the corresponding amines. The solid-state structure of **18** was determined unequivocally using single-crystal X-ray diffraction analysis (for details, see the Supporting Information).

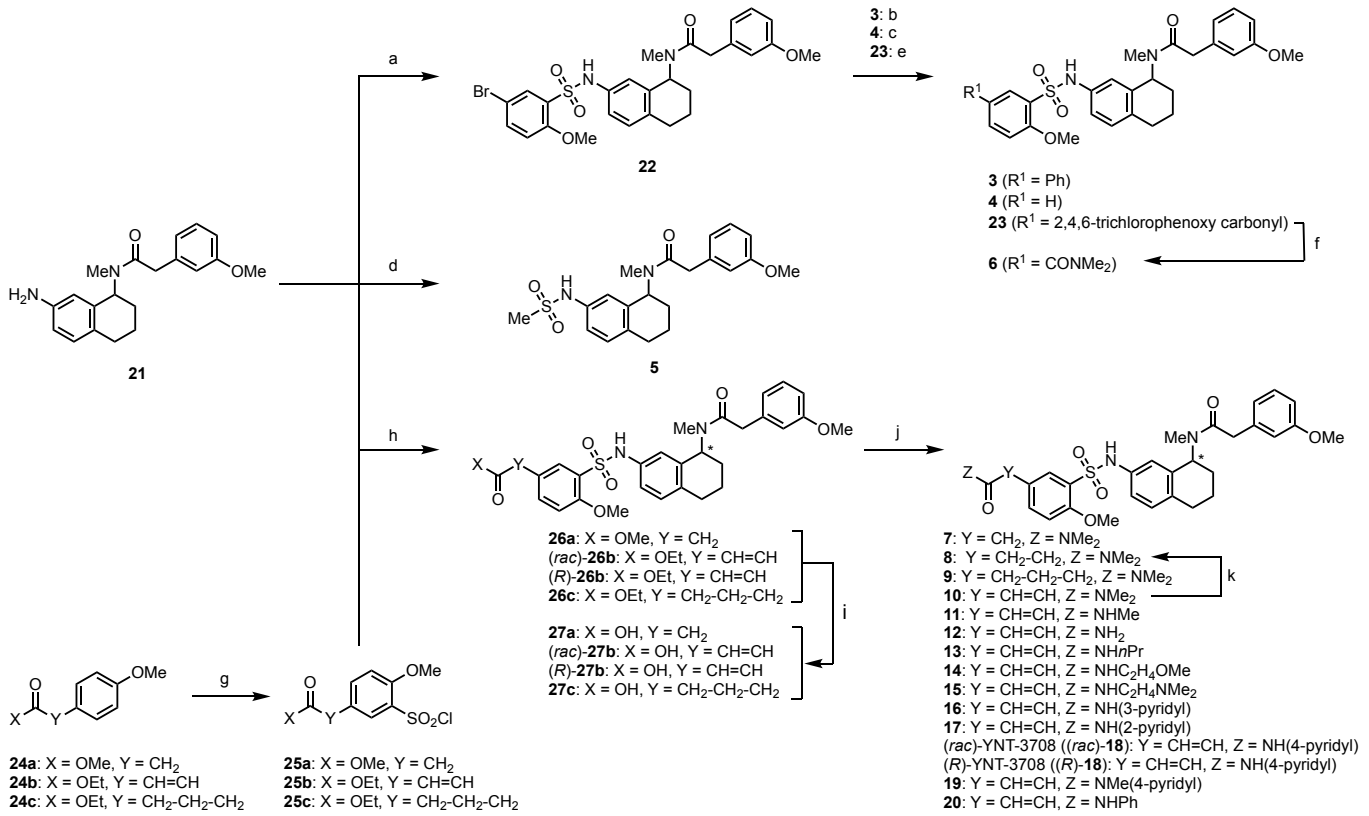

Scheme 1. Reagents and conditions for the synthesis of assayed compounds: (a) 5-bromo-2-methoxysulfonyl chloride, pyridine, CH_2Cl_2, r.t., 99%; (b) phenylboronic acid, $Pd(PPh_3)_4$, 2.5 M Na_2CO_3 aq., DME, reflux, 55%; (c) H_2, Pd/C, MeOH/EtOAc, r.t., 78%; (d) methanesulfonyl chloride, pyridine, CH_2Cl_2, r.t., 81%; (e) 2,4,6-trichlorophenyl formate, $Pd(OAc)_2$, Xantphos, DBU, toluene, 80 °C; (f) dimethylamine hydrochloride, Et_3N, DMAP, THF, r.t. 30% over 2 steps; (g) chlorosulfonic acid, CH_2Cl_2, 0 °C, then $SOCl_2$, DMF, reflux, 45% for **25a**, 83% for **25b**, and 95% for **25c**; (h) **25a**–**c**, pyridine, CH_2Cl_2, 74% for (*rac*)-**26a**, 95% for **26b**, and 92% for **26c**; (i) NaOH aq. or LiOH aq., THF, r.t., 90% for (*rac*)-**27a**, 78% for (*rac*)-**27b**, 99% for **27c**; (j) corresponding amines (Z–H), COMU or HATU, DIPEA, DMF, r.t., 97% for **7**, 96% for **9**; 56% for **10**, 98% for **11**, 68% for **12**, 75% for **13**, 87% for **14**, 65% for **15**, 53% for **16**, 40% for **17**, 81% for (*rac*)-YNT-3708 ((*rac*)-**18**), 62% for (*R*)-YNT-3708 ((*R*)-**18**) in 2 steps, 73% for **19**, and 80% for **20**; (k) H_2, Pd/C, MeOH, r.t., 82%.

In our previous study, separation of the enantiomers of tetralin derivative (*rac*)-**2** identified the (*R*)-tetralin core structure as a eutomer structure for both receptors.[33] While we also separated the optical isomers of (*rac*)-**18** using preparative chiral HPLC, the individual isomers did not crystallize, whereas (*rac*)-**18** crystallized. Therefore, the absolute stereochemistry of each isomer was determined by asymmetric synthesis of the (*R*)-isomer from optically pure (*R*)-**21**[33] according to the same procedure as (*rac*)-**18** (Scheme 1) and comparison of the optical properties. Consistent with our previous research, (*R*)-

159 **18** showed a *ca*. two-fold increase in agonist activity for both receptors compared to (*rac*)-**18**, while (*S*)-**18**
160 showed a significant decrease in agonist activity for both receptors (Table 3). Importantly, the eutomer (*R*)-
161 **18** showed 290-fold weaker OX_2R-agonist activity than (*R*)-**2**, but a 1.8-fold more potent OX_1R-agonist
162 activity than (*R*)-**2**, leading to a significant improvement in OX_1R selectivity for (*R*)-**2** (OX_2R/OX_1R = 22.5
163 *vs.* 0.042). Given that the active-state structure of OX_1R bound with its agonist has not yet been elucidated,
164 it is difficult to estimate the binding modes of (*R*)-**18**. However, these results suggested that the tetralin-
165 phenylacetamide unit with an (*R*)-stereochemistry is important for the strong activation of both receptors,
166 while the sulfonamide unit plays a more important role in the receptor selectivity. This is probably due to
167 the differences in the binding pocket around the biphenyl group. The binding pockets of OX_1R and OX_2R
168 differ in only two residues ($S103^{2.61}/T111^{2.61}$ and $A127^{3.33}/T135^{3.33}$), which give rise to a larger volume in
169 the OX_1R-binding pocket than that of OX_2R.[28] While the rigid biphenyl moiety can potentially occupy the
170 binding pocket of both receptors, the cinnamoyl amide moiety can be expected to be unstable in the slightly
171 tighter binding pocket of OX_2R due to lack of key hydrophobic interactions between the aromatic A-ring
172 and OX_2R and/or on account of the flexibility of the acrylamide unit.

173
174 **Table 3.** Orexin receptor-agonist activity of each enantiomer of (*rac*)-YNT-3708 (**18**)

Comp.	Structure	EC_{50} (nM) [E_{max} (%)[a]]		Selectivity (OX_2R/OX_1R)
		OX_1R	OX_2R	
(*rac*)-**18**	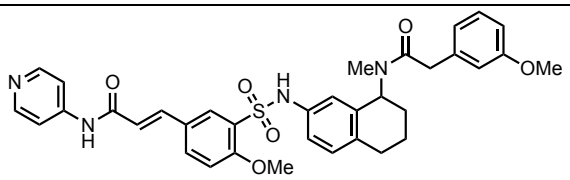	15.0 [104]	277 [98.6]	19.0
(*S*)-**18**	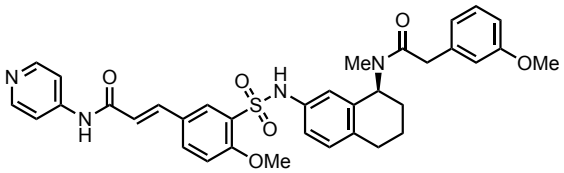	3,595 [71.2[b]]	1,661 [47.4[b]]	0.46
(*R*)-**18**	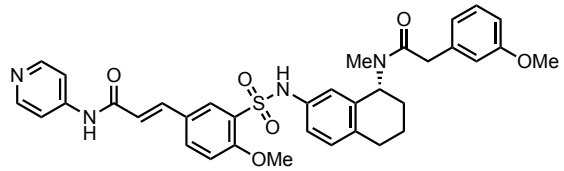	7.47 [101]	168 [168]	22.5

175 [a] E_{max} expressed as a percentage of OXA maximum. [b] Value obtained at 10 μM.
176

177 **In vivo Pharmacology of (*R*)-YNT-3708 ((*R*)-18)**

178 With the first OX_1R-selective agonist in hand, we then assessed the potential of the OX_1R-selective
179 small-molecule agonist (*R*)-**18** for *in vivo* experiments. Several pharmacological studies using 1-SORA and
180 genetic studies have suggested that the reinforcing effect of OXA is mainly mediated by OX_1R rather than
181 by OX_2R.[35] Moreover, our group has recently reported that the OX_2R-selective peptide AL-OXB does not
182 show any preference in a conditioned place-preference (CPP) test.[14] However, the direct involvement of
183 receptor-selective activation in the reward system has not yet been investigated using selective small-
184 molecule agonists. Thus, we first performed a CPP test using the OX_1R-selective agonist (*R*)-**18**, OX_2R-
185 selective agonist (*S*)-**2**, and OX_1R/OX_2R dual agonist (*R*)-**2** to clarify the involvement of OX_1R-selective
186 activation in the reward system. The subcutaneous (s.c.) administration of OX_2R-selective agonist (*S*)-**2** did
187 not induce a place preference (Figure 3A), while dual agonist (*R*)-**2** and OX_1R-selective agonist (*R*)-**18**
188 produced a detectable place preference at 40 mg/kg (Figure 3B and 3C), although their reinforcing effect
189 was significantly weaker than that of the typical addictive drug cocaine, especially for (*R*)-**18**. The (*R*)-**18**-
190 induced place preference in wild-type mice was significantly reduced in OX_1R-knockout mice (Figure 3D).
191 These results indicate, as previously reported, that OX_1R-selective activation induces reinforcing effects,
192 albeit that these effects might not necessarily be as strong as those of existing addictive drugs; the
193 clarification of this point requires further investigations that are beyond the scope of the present study.
194 Next, we evaluated the antinociceptive effect of (*R*)-**18** using the mouse tail-flick test. OX_1R are
195 localized in areas of the brain and spinal cord associated with nociceptive processing,[36,37] and stimulation
196 of the lateral hypothalamus area, where orexin neurons are located, produces analgesia.[38] Additionally,
197 several studies have shown that the central administration of the endogenous dual agonist OXA, but not the
198 endogenous OX_2R-selective agonist OXB, shows an antinociceptive effect in rats and mice, suggesting that
199 the OX_1R system plays an important role in pain modulation.[37] The subcutaneous administration of OX_1R-
200 selective agonist (*R*)-**18** showed a dose-dependent antinociceptive effect in the mouse-tail-flick test,
201 whereby the maximum effect is observed 30 min after administration (Figure 4). These data suggest that
202 OX_1R-selective agonists can be expected to be useful as a new class of antinociceptive agents.
203

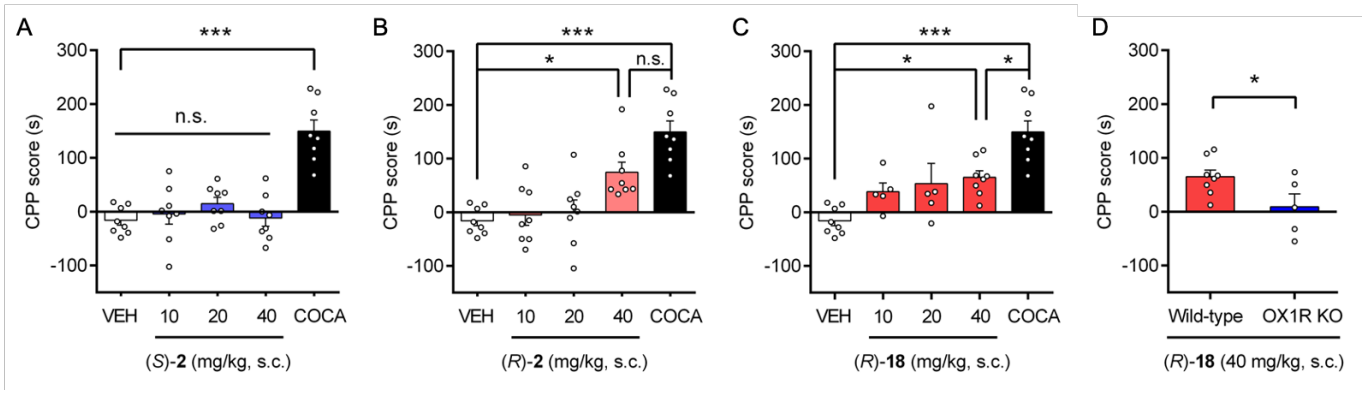

Figure 3. Effects of orexin receptor agonists in a conditioned place-preference (CPP) test. (A–C) Effects of different doses of (*S*)-**2** (B), (*R*)-**2** (C), and (*R*)-**18** on the CPP score. The same CPP data for vehicle and cocaine (COCA) injections are presented in (A), (B), and (C). Data represent the mean values ± SEM from 8 mice for 10, 20, and 40 mg/kg (*S*)-**2**, 8 mice for 10, 20, and 40 mg/kg (*R*)-**2**, 5 mice for 10 and 20 mg/kg (*R*)-**18**, 8 mice for 40 mg/kg (*R*)-**18**, 8 mice for the vehicle, and 8 mice for 20 mg/kg cocaine. Statistical analysis: one-way ANOVA followed by Tukey's multiple comparisons test. (D) Effects of (*R*)-**18** at 40 mg/kg in wild-type mice and OX_1R-knockout mice. The same CPP data for 40 mg/kg (*R*)-**18** injections are presented in (C) and (D). Data represent the mean values ± SEM from 5 mice for 40 mg/kg (*R*)-**18** in OX_1R-knockout mice and 8 mice for 40 mg/kg (*R*)-**18** in wild-type mice. Statistical analysis: unpaired Student's *t*-test.

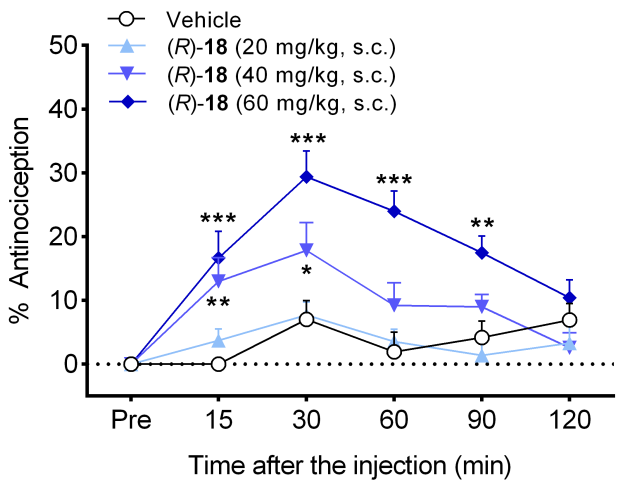

Figure 4. Antinociceptive effect of (*R*)-**18** in a tail-flick test. Time course of analgesic effect induced by different doses of (*R*)-**18** (20–60 mg/kg, s.c.) in the mouse-tail-flick test. Data represent the mean value ± SEM from 9 mice for 20 and 40 mg/kg (*R*)-**18** and 8 mice for 60 mg/kg (*R*)-**18** and vehicle. Statistical analysis: two-way ANOVA followed by Dunnett test.

220
221 **Conclusions**

222 In conclusion, we have discovered a potent and centrally active OX_1R-selective agonist, YNT-
223 3708 (**18**), through a structure–activity relationship study focusing on the biphenyl moiety based on the
224 structure of a tetralin-type agonist **2**. The replacement of the biphenyl unit with a vinylogous phenyl scaffold
225 enhances the potency toward OX_1R but not OX_2R, which is important to achieve selective interactions with
226 OX_1R. After enantiomer separation, (*R*)-YNT-3708 ((*R*)-**18**) exhibited superior OX_1R-selective agonist
227 activity. The peripheral (subcutaneous) administration of (*R*)-**18** induced a weak reinforcing effect in a
228 conditioned place-preference (CPP) test and an antinociceptive effect in a mouse-tail-flick test. These
229 results suggest that OX_1R-selective agonists can be expected to serve as a new class of useful
230 antinociceptive agents. To the best of our knowledge, OX_1R-selective agonists have not been disclosed so
231 far (including patents), even though several OX_2R-selective- and dual orexin receptor-agonists have already
232 been reported. OX_1R plays prominent roles in the physiological events such as not only reward and
233 analgesia, but also sleep–wakefulness, feeding behavior, energy homeostasis, emotions, and the autonomic
234 nervous system. Our findings thus contribute not only to the development of medicinal chemistry targeting
235 orexin receptors, but also to further investigations for the elucidation of the physiological and pathogenetic
236 functions of OX_1R.

237

238 **Experimental Section**

239 **Chemistry**

240 All reagents and solvents were purchased from the following commercial suppliers: Tokyo
241 Chemical Industry, Sigma-Aldrich, Inc., Kanto Chemical Co., Inc., Wako Pure Chemical Ind., Ltd. and
242 Nacalai Tesque. All commercially available chemicals and solvents were used as received. In general,
243 reaction mixtures were magnetically stirred at the indicated temperature under an argon atmosphere. The
244 synthetic compounds described in this study were checked with analytical thin-layer chromatography (TLC,
245 Merck Co., Ltd., Kieselgel 60 F_{254}, 0.25 mm), visualized under UV light at 254 nm and phosphomolybdic
246 acid in an aqueous solution of sulfuric acid, Hanessian stain, ninhydrin, or *p*-anisaldehyde followed by
247 heating. Column chromatography was carried out on silica gel (a: spherical, neutral, 40–50 μm, Kanto

248 Chemical Co., Japan; b: spherical, neutral, CHROMATOREX PSQ60B, 60 μm, Fuji Silysia Chemical Ltd.).
249 Preparative TLC was performed on Kieselgel 60 F_{254} (0.50 mm) plates (Merck Co., Ltd.). Infrared (IR)
250 spectra were recorded on a JASCO FT/IR-4100Plus. Nuclear magnetic resonance (NMR) spectra were
251 obtained on a JEOL JNM-ECS 400 (^{1}H: 400 MHz; ^{13}C: 101 MHz). NMR chemical shifts are given in ppm
252 using tetramethylsilane (TMS, δ 0 ppm) as the reference for the ^{1}H NMR spectra and $CDCl_3$ (δ 77.16 ppm)
253 for the ^{13}C NMR spectra. Some compounds were observed as a mixture of rotamers. Mass spectra (MS)
254 were obtained on a JEOL JMS-T100LP spectrometer. Elemental analyses were performed with on a J-
255 SCIENCE LAB microcorder JM10. The purity (≥95%) of the assayed compounds was determined using
256 analytical HPLC. Analytical HPLC was performed on an ACQUITY UPLC system (Waters Co., Ltd)
257 equipped with an ACQUITY UPLC BEH C18 column (1.7 μm, 50 mm × 2.1 mm), with PDA detection at
258 254 nm at a column temperature of 40 °C. Optical rotations were measured using an Anton Paar MCP 100
259 Polarimeter.

260 **Preparation of (*R*)-YNT-3708 ((*R*)-18)**

261 **Ethyl (*E*)-3-(3-(chlorosulfonyl)-4-methoxyphenyl)acrylate (25b)**

262 Chlorosulfonic acid (0.321 mL, 4.87 mmol) was added to a solution of ethyl 4-methoxycinnamate (201 mg,
263 0.975 mmol) in CH_2Cl_2 (5.0 mL) at 0 °C, before the solution was stirred for 30 min. Subsequently, $SOCl_2$
264 (0.703 mL, 9.75 mmol) and DMF (3.75 μL, 0.0487 mmol) were added to the reaction mixture, before the
265 mixture was heated to reflux for 10 min. Then, the reaction mixture was poured into water and extracted
266 with $CHCl_3$ (20, 20, 10, and 10 mL). The combined organic layers were dried over Na_2SO_4 and filtered
267 before the filtrate was concentrated under reduced pressure. The crude residue was purified by column
268 chromatography on silica gel (0–25% EtOAc in hexane) to afford **25b** (247 mg, 83%) as a white solid. IR
269 (neat): 2983, 1710, 1603, 1499, 1370, 1173 cm^{-1}. ^{1}H NMR (400 MHz, $CDCl_3$) δ 1.34 (t, *J* = 7.2 Hz, 3H),
270 4.10 (s, 3H), 4.27 (q, *J* = 7.2 Hz, 2H), 6.41 (d, *J* = 16.0 Hz, 1H), 7.15 (d, *J* = 8.7 Hz, 1H), 7.62 (d, *J* = 16.0
271 Hz, 1H), 7.81 (dd, *J* = 8.7, 2.3 Hz, 1H), 8.12 (d, *J* = 2.3 Hz, 1H). ^{13}C NMR (101 MHz, $CDCl_3$) δ 14.4, 57.1,
272 60.9, 113.8, 119.4, 127.4, 129.2, 132.4, 136.4, 141.4, 158.3, 166.5. EA Anal. Calcd for
273 $C_{13}H_{12}O_5SCl \cdot 0.2H_2O$: C, 46.74; H, 4.38; N, 0.00. Found: C, 46.78; H, 4.26; N, 0.00.

Ethyl (*R*,*E*)-3-(4-methoxy-3-(*N*-(8-(2-(3-methoxyphenyl)-*N*-methylacetamido)-5,6,7,8-tetrahydronaphthalen-2-yl)sulfamoyl)phenyl)acrylate ((*R*)-26b)

A mixture of **21** (41.0 mg, 0.126 mmol) and **25b** (40.4 mg, 0.133 mmol) in CH_2Cl_2 (0.80 mL) was stirred with pyridine (0.20 mL) for 2 h at room temperature under an argon atmosphere. The reaction mixture was quenched with sat. $NaHCO_3$ aq. (30 mL) and extracted with $CHCl_3$ (30, 15, and 5 mL). The combined organic layers were washed with brine (30 mL), dried over Na_2SO_4 and filtered before the filtrate was concentrated under reduced pressure. The thus obtained crude material was used for the next reaction without further purification.

(*R*,*E*)-3-(4-Methoxy-3-(*N*-(8-(2-(3-methoxyphenyl)-*N*-methylacetamido)-5,6,7,8-tetrahydronaphthalen-2-yl)sulfamoyl)phenyl)acrylic acid ((*R*)-27b)

A solution of crude (*R*)-**26b** in THF (3.0 mL) was treated with 1 M NaOH aq. (3.0 mL) at room temperature under an argon atmosphere, and the mixture was stirred for 15 h. Then, the reaction mixture was quenched by the addition of 1 M HCl aq. (5.0 mL) and extracted with $CHCl_3$ (30, 15, and 5 mL). The combined organic layers were dried over Na_2SO_4 and filtered before the filtrate was concentrated under reduced pressure. The thus obtained crude product was used for the next reaction without further purification.

(*R*,*E*)-3-(4-Methoxy-3-(*N*-(8-(2-(3-methoxyphenyl)-*N*-methylacetamido)-5,6,7,8-tetrahydronaphthalen-2-yl)sulfamoyl)phenyl)-*N*-(pyridin-4-yl)acrylamide ((*R*)-YNT-3708; (*R*)-18)

A mixture of (*R*)-**27b** (1.22 g, 2.16 mmol), 4-aminopyridine (308 mg, 3.27 mmol), HATU (989 mg, 2.60 mmol), and DIPEA (739 μL, 4.32 mmol) in DMF (10 mL) was stirred for 22 h at room temperature under an argon atmosphere. The reaction mixture was diluted with sat. $NaHCO_3$ aq. (100 mL) and extracted with $CHCl_3$ (200, 100, 100, and 100 mL). The combined organic layers were dried over Na_2SO_4 and filtered before the filtrate was concentrated under reduced pressure. The thus obtained crude residue was purified by column chromatography on silica gel (0–9% MeCN in $CHCl_3$) and preparative TLC (5% MeOH in $CHCl_3$ and 9% MeOH in $CHCl_3$) to afford (*R*)-**18** (851 mg, 62%) as a colorless amorphous solid. IR (neat): 2936, 1629, 1599, 1496, 1156 cm^{-1}. ^1H NMR (400 MHz, $CDCl_3$): δ (ppm) 1.45–2.11 (m, 4H), 2.36 (s, 0.9H), 2.52–2.79 (m, 2H), 2.86 (s, 2.1H), 3.51–4.12 (m, 8H), 5.00–5.17 (m, 0.3H), 5.71–5.92 (m, 0.7H), 6.34 (d, J = 15.6 Hz, 0.7H), 6.55–6.83 (m, 2.3H), 6.83–7.05 (m, 4H), 7.16 (t, J = 7.8 Hz, 1H), 7.25–7.29

301 (m, 1H), 7.38–7.60 (m, 4H), 8.13 (d, J = 2.3 Hz, 0.7H), 8.24 (d, J = 1.8 Hz, 0.3H), 8.32–8.53 (m, 2H), 9.70
302 (s, 0.7H), 10.01 (s, 0.3H). The NH peak was not observed. ^{13}C NMR (100 MHz, $CDCl_3$): δ (ppm) 22.0,
303 27.0, 28.2, 28.7, 28.8, 31.6, 40.9, 40.9, 53.7, 55.1, 55.4, 56.8, 57.5, 112.0, 112.4, 112.6, 112.8, 113.7, 113.9,
304 114.0, 114.6, 115.3, 116.2, 117.1, 118.2, 121.5, 121.9, 123.4, 123.7, 126.3, 127.5, 128.0, 128.5, 128.6,
305 128.9, 130.1, 130.3, 130.5, 130.7, 133.9, 134.1, 135.4, 135.7, 135.8, 136.1, 136.2, 136.2, 136.5, 136.6,
306 138.9, 139.4, 146.9, 146.9, 149.1, 149.5, 157.6, 160.0, 164.9, 165.3, 172.2, 173.4. HR-MS (ESI): *m*/*z*
307 $[M+H]^+$ calcd for $C_{35}H_{37}N_4O_6S$: 641.24338, found: 641.24228; $[\alpha]_{589}^{20}$ = +46.131 (c = 0.336, $CHCl_3$).
308 To improve the solubility in aqueous solution for an *in vivo* assay, (*R*)-**18** was converted into its
309 hydrochloric-acid salt.
310 (*R*)-**18**·HCl: Anal. Calcd for $C_{35}H_{36}N_4O_6$·HCl·3.4H_2O: C, 56.93; H, 5.98; N, 7.59. Found: C, 56.90; H,
311 5.78; N, 7.45.
312 The preparation methods for other tested compounds are described in the Supporting Information.
313
314 **Calcium-mobilization assay**
315 Chinese hamster ovary (CHO)-K1 cells stably expressing human OX_1R ($CHOOX_1R$) or OX_2R
316 ($CHOOX_2R$) were seeded in a 96-well plate (10,000 cells/well) and then incubated with 5% FBS/DMEM
317 at 37 °C for 48 h. After the incubation, the cells were loaded with 5 μM of the fluorescent calcium indicator
318 Fura 2-AM (Cayman Chemical, Michigan, USA) in Hanks balanced salt solution (HBSS) including 20 mM
319 HEPES, 2.5 mM Probenecid, 0.04% Cremophor EL, and 0.1% BSA at 37 °C for 1 h. The cells were washed
320 once, and 75 μL of HBSS buffer was added. The cells were then treated with 25 μL of various
321 concentrations of test compounds or orexin A. The increase in intracellular Ca^{2+} concentration was
322 measured based on the ratio of emission fluorescence at 510 nm with excitation at 340 nm or 380 nm using
323 the Functional Drug Screening System 7000 system (Hamamatsu Photonics, Shizuoka, Japan). Sigmoidal
324 concentration–response curves were produced using the software GraphPad Prism (version 6.05; GraphPad
325 Software Inc., La Jolla, CA, USA). The agonist stimulation of all test compounds was determined by
326 normalizing all values to the maximum response (E_{max}) of the sigmoidal curve produced by orexin A. The
327 values of E_{max} and half maximal effective concentration (EC_{50}) for all test compounds were obtained from

328 the average of 1–2 independent experiments. For comparison of the stereoisomers of **18**, the values of E_{max}
329 and EC_{50} for (*rac*)-, (*S*)-, and (*R*)-**18** were obtained from individual experiments (Table 3).
330

331 **Conditioned place-preference (CPP) test**

332 The conditioned place-preference (CPP) test was performed according to previous reports.[35,39] The
333 measuring vessel was divided into two compartments of equal size. The surface of one compartment was
334 white and rough, while that of the other was black and smooth. The test involved three phases: a (i) pre-
335 test session, a (ii) conditioning session, and a (iii) post-test session. In the pre-test session, mice that had
336 not been treated with either the test compounds or vehicle were placed in the measuring vessel, and the
337 time spent by the mice in each compartment (total: 15 minutes) was measured. Next, conditioning sessions
338 were conducted for six days, and either the test compounds (dissolved in a solution of 5% DMSO, 5%
339 Cremophor EL®, 20% PEG400, and 70% 1% Soluplus® aq.) or the vehicle was administered by s.c.
340 injection each day. After administration of the test compounds, the animals were placed in the compartment
341 opposite that in which they spent the most time in the pre-test session for 1 h. On alternating days, the same
342 animals instead received the vehicle, and were placed in the other compartment for 1 h. On the day after
343 the final conditioning session, the post-test session was conducted under the same conditions as the pre-test
344 session. The CPP score was defined as the time spent in the drug-associated side of the box after drug
345 conditioning subtracted from the time spent there before drug conditioning.
346

347 **Tail-flick test**

348 Tail-flick tests were performed to assess test-compounds-induced analgesic effects. The tail-flick response
349 was evoked by thermal stimulation to the mouse tail and the latencies were determined by using a recording
350 equipment (model 336, IITC Inc. Life Science, Woodland Hills, CA, USA). To prevent tail-tissue damage,
351 the cut-off time was set to 15 s.[40,41] The intensity of the thermal stimulus was adjusted to achieve an average
352 basal latency of approximately 4 s in naive mice. Post-injection latency was measured at 15, 30, 60, 90 and
353 120 min after subcutaneous treatment of test compounds (dissolved in a solution of 5% DMSO, 5%

354 Cremophor EL®, 20% PEG400, and 70% 1% Soluplus® aq.) or vehicle. The analgesic percentage is defined
355 as 100 x (post-injection test latency – basal latency) / (cut-off time – basal latency).
356

357 **Supporting Information**

358 Preparation of tested compounds, enantiomer separation, chiral-column analysis, HPLC traces, and X-ray
359 crystallography (PDF)
360 Molecular formula strings (CSV)
361

362 **Author Information**

363 **Corresponding Authors**

364 **Hiroshi Nagase –** *International Institute for Integrative Sleep Medicine; Graduate School of Pure and*
365 *Applied Sciences, University of Tsukuba, 1-1-1 Tennodai, Tsukuba, Ibaraki 305-8575, Japan*; Email:
366 nagase.hiroshi.gt@u.tsukuba.ac.jp
367 **Tsuyoshi Saitoh –** *International Institute for Integrative Sleep Medicine; Graduate School of*
368 *Comprehensive Human Sciences, University of Tsukuba, 1-1-1 Tennodai, Tsukuba, Ibaraki 305-8575,*
369 *Japan*; Email: tsuyoshi-saito.gf@u.tsukuba.ac.jp

370 **Authors**

371 **Keita Iio –** *International Institute for Integrative Sleep Medicine; Graduate School of Pure and Applied*
372 *Sciences, University of Tsukuba, 1-1-1 Tennodai, Tsukuba, Ibaraki 305-8575, Japan*
373 **Kao Hashimoto** – *International Institute for Integrative Sleep Medicine; Graduate School of*
374 *Comprehensive Human Sciences, University of Tsukuba, 1-1-1 Tennodai, Tsukuba, Ibaraki 305-8575,*
375 *Japan*
376 **Yasuyuki Nagumo** – *International Institute for Integrative Sleep Medicine, University of Tsukuba, 1-1-1*
377 *Tennodai, Tsukuba, Ibaraki 305-8575, Japan*
378 **Taisei Hasegawa** – *International Institute for Integrative Sleep Medicine; Graduate School of Pure and*
379 *Applied Sciences, University of Tsukuba, 1-1-1 Tennodai, Tsukuba, Ibaraki 305-8575, Japan*

380 **Mao Amezawa** – *International Institute for Integrative Sleep Medicine; Graduate School of Pure and*
381 *Applied Sciences, University of Tsukuba, 1-1-1 Tennodai, Tsukuba, Ibaraki 305-8575, Japan*
382 **Naoshi Yamamoto** – *International Institute for Integrative Sleep Medicine, University of Tsukuba, 1-1-1*
383 *Tennodai, Tsukuba, Ibaraki 305-8575, Japan*
384 **Noriki Kutsumura** – *International Institute for Integrative Sleep Medicine; Graduate School of Pure and*
385 *Applied Sciences; Graduate School of Comprehensive Human Sciences, University of Tsukuba, 1-1-1*
386 *Tennodai, Tsukuba, Ibaraki 305-8575, Japan*
387 **Katsuhiko Takeuchi** – *National Institute of Advanced Industrial Science and Technology (AIST), Tsukuba*
388 *Central 5, 1-1-1 Higashi, Tsukuba 305-8565, Ibaraki, Japan*
389 **Yukiko Ishikawa** – *International Institute for Integrative Sleep Medicine, University of Tsukuba, 1-1-1*
390 *Tennodai, Tsukuba, Ibaraki 305-8575, Japan*
391 **Masashi Yanagisawa** – *International Institute for Integrative Sleep Medicine; R&D Center for Frontiers*
392 *of Mirai in Policy and Technology (F-MIRAI), University of Tsukuba, 1-1-1 Tennodai, Tsukuba, Ibaraki,*
393 *305-8575, Japan; Department of Molecular Genetics, University of Texas Southwestern Medical Center,*
394 *Dallas, TX75390, United States*
395

396 **Author Contributions**

397 †These authors contributed equally to this work.

398 The manuscript was written through contributions of all authors. All authors approved of the final version
399 of the manuscript.

400

401 **Notes**

402 The authors declare no competing financial interest.

403

404 **Acknowledgements**

405 This work was supported by JSPS KAKENHI grant 19H03428, 20K05743, and 21B209 (to T.S.) as well
406 as 16H05098 and 20H03361 (to H.N., Y.N., T.S.), the Japan Foundation for Applied Enzymology (16H007

407 to T.S.), AMED under grant number JP21zf0127005, and a grant of collaborative research between the
408 University of Tsukuba and the Toyota Motor Corporation. IIIS is supported by the World Premier
409 International Research Center Initiative (WPI), Japan.

410

411 **Abbreviations**

412 1-SORA, selective orexin 1 receptor-antagonist; AL-OXB, [Ala[11], D-Leu[15]]-orexin-B; ANOVA, analysis
413 of variance; CHO, Chinese hamster ovary; COCA, cocaine; COMU, 1-[(1-(cyano-2-ethoxy-2-
414 oxoethylideneaminooxy) dimethylaminomorpholino)] uronium hexafluorophosphate; CPP, conditioned
415 place-preference; DBU, 1,8-diazabicyclo[5.4.0]undec-7-ene; DIPEA, *N*,*N*-diisopropylethylamine; EtOAc,
416 ethyl acetate; HATU, 1-[bis(dimethylamino)methylene]-1*H*-1,2,3-triazolo[4,5-*b*]pyridinium 3-oxide
417 hexafluorophosphate; MeOH, methanol; OXA, orexin A; OXB, orexin B; OXR, orexin receptor; OX_1R,
418 orexin 1 receptor; OX_2R, orexin 2 receptor; *rac*, racemic; SEM, standard error of the mean; Xantphos, 4,5-
419 bis(diphenylphosphino)-9,9-dimethylxanthene.

420

421 **References**

422 (1) Sakurai, T.; Amemiya, A.; Ishii, M.; Matsuzaki, I.; Chemelli, R. M.; Tanaka, H.; Williams, S. C.;
423 Richardson, J. A.; Kozlowski, G. P.; Wilson, S.; Arch, J. R. S.; Buckingham, R. E.; Haynes, A. C.;
424 Carr, S. A.; Annan, R. S.; McNulty, D. E.; Liu, W. S.; Terrett, J. A.; Elshourbagy, N. A.; Bergsma, D.
425 J.; Yanagisawa, M. Orexins and Orexin Receptors: A Family of Hypothalamic Neuropeptides and G
426 Protein-Coupled Receptors That Regulate Feeding Behavior. *Cell* **1998**, *92* (4), 573–585.

427 (2) de Lecea, L.; Kilduff, T. S.; Peyron, C.; Gao, X.; Foye, P. E.; Danielson, P. E.; Fukuhara, C.;
428 Battenberg, E. L.; Gautvik, V. T.; Bartlett, F. S., 2nd; Frankel, W. N.; van den Pol, A. N.; Bloom, F.
429 E.; Gautvik, K. M.; Sutcliffe, J. G. The Hypocretins: Hypothalamus-Specific Peptides with
430 Neuroexcitatory Activity. *Proc. Natl. Acad. Sci. U. S. A.* **1998**, *95* (1), 322–327.

431 (3) Marcus, J. N.; Aschkenasi, C. J.; Lee, C. E.; Chemelli, R. M.; Saper, C. B.; Yanagisawa, M.; Elmquist,
432 J. K. Differential Expression of Orexin Receptors 1 and 2 in the Rat Brain. *J. Comp. Neurol.* **2001**,
433 *435* (1), 6–25.

434 (4) Sakurai, T. The Role of Orexin in Motivated Behaviours. *Nat. Rev. Neurosci.* **2014**, *15* (11), 719–731.

435 (5) Lin, L.; Faraco, J.; Li, R.; Kadotani, H.; Rogers, W.; Lin, X.; Qiu, X.; de Jong, P. J.; Nishino, S.;
436 Mignot, E. The Sleep Disorder Canine Narcolepsy Is Caused by a Mutation in the Hypocretin (Orexin)
437 Receptor 2 Gene. *Cell* **1999**, *98* (3), 365–376.
438 (6) Chemelli, R. M.; Willie, J. T.; Sinton, C. M.; Elmquist, J. K.; Scammell, T.; Lee, C.; Richardson, J.
439 A.; Williams, S. C.; Xiong, Y.; Kisanuki, Y.; Fitch, T. E.; Nakazato, M.; Hammer, R. E.; Saper, C. B.;
440 Yanagisawa, M. Narcolepsy in Orexin Knockout Mice: Molecular Genetics of Sleep Regulation. *Cell*
441 **1999**, *98* (4), 437–451.
442 (7) Willie, J. T.; Chemelli, R. M.; Sinton, C. M.; Tokita, S.; Williams, S. C.; Kisanuki, Y. Y.; Marcus, J.
443 N.; Lee, C.; Elmquist, J. K.; Kohlmeier, K. A.; Leonard, C. S.; Richardson, J. A.; Hammer, R. E.;
444 Yanagisawa, M. Distinct Narcolepsy Syndromes in Orexin Receptor-2 and Orexin Null Mice:
445 Molecular Genetic Dissection of Non-REM and REM Sleep Regulatory Processes. *Neuron* **2003**, *38*
446 (5), 715–730.
447 (8) Sakurai, T. The Neural Circuit of Orexin (Hypocretin): Maintaining Sleep and Wakefulness. *Nat. Rev.*
448 *Neurosci.* **2007**, *8* (3), 171–181.
449 (9) Hasegawa, E.; Miyasaka, A.; Sakurai, K.; Cherasse, Y.; Li, Y.; Sakurai, T. Rapid Eye Movement Sleep
450 Is Initiated by Basolateral Amygdala Dopamine Signaling in Mice. *Science* **2022**, *375* (6584), 994–
451 1000.
452 (10) Mieda, M.; Hasegawa, E.; Kisanuki, Y. Y.; Sinton, C. M.; Yanagisawa, M.; Sakurai, T. Differential
453 Roles of Orexin Receptor-1 and -2 in the Regulation of Non-REM and REM Sleep. *J. Neurosci.* **2011**,
454 *31* (17), 6518–6526.
455 (11) Morairty, S. R.; Revel, F. G.; Malherbe, P.; Moreau, J.-L.; Valladao, D.; Wettstein, J. G.; Kilduff, T.
456 S.; Borroni, E. Dual Hypocretin Receptor Antagonism Is More Effective for Sleep Promotion than
457 Antagonism of Either Receptor Alone. *PLoS One* **2012**, *7* (7), e39131.
458 (12) Sakurai, T. Orexins and Orexin Receptors: Implication in Feeding Behavior. *Regul. Pept.* **1999**, *85* (1),
459 25–30.
460 (13) Harris, G. C.; Wimmer, M.; Aston-Jones, G. A Role for Lateral Hypothalamic Orexin Neurons in
461 Reward Seeking. *Nature* **2005**, *437* (7058), 556–559.

462 (14) Yamamoto, H.; Nagumo, Y.; Ishikawa, Y.; Irukayama-Tomobe, Y.; Namekawa, Y.; Nemoto, T.;
463 Tanaka, H.; Takahashi, G.; Tokuda, A.; Saitoh, T.; Nagase, H.; Funato, H.; Yanagisawa, M. OX2R-
464 Selective Orexin Agonism Is Sufficient to Ameliorate Cataplexy and Sleep/Wake Fragmentation
465 without Inducing Drug-Seeking Behavior in Mouse Model of Narcolepsy. *PLoS One* **2022**, *17* (7),
466 e0271901.
467 (15) Yamamoto, T.; Nozaki-Taguchi, N.; Chiba, T. Analgesic Effect of Intrathecally Administered Orexin-
468 A in the Rat Formalin Test and in the Rat Hot Plate Test. *Br. J. Pharmacol.* **2002**, *137* (2), 170–176.
469 (16) Mobarakeh, J. I.; Takahashi, K.; Sakurada, S.; Nishino, S.; Watanabe, H.; Kato, M.; Yanai, K.
470 Enhanced Antinociception by Intracerebroventricularly and Intrathecally-Administered Orexin A and
471 B (Hypocretin-1 and -2) in Mice. *Peptides* **2005**, *26* (5), 767–777.
472 (17) Ho, Y.-C.; Lee, H.-J.; Tung, L.-W.; Liao, Y.-Y.; Fu, S.-Y.; Teng, S.-F.; Liao, H.-T.; Mackie, K.; Chiou,
473 L.-C. Activation of Orexin 1 Receptors in the Periaqueductal Gray of Male Rats Leads to
474 Antinociception via Retrograde Endocannabinoid (2-Arachidonoylglycerol)-Induced Disinhibition. *J.*
475 *Neurosci.* **2011**, *31* (41), 14600–14610.
476 (18) Yamanaka, A.; Beuckmann, C. T.; Willie, J. T.; Hara, J.; Tsujino, N.; Mieda, M.; Tominaga, M.;
477 Yagami, K. I.; Sugiyama, F.; Goto, K.; Yanagisawa, M.; Sakurai, T. Hypothalamic Orexin Neurons
478 Regulate Arousal According to Energy Balance in Mice. *Neuron* **2003**, *38* (5), 701–713.
479 (19) Sakurai, T.; Mieda, M. Connectomics of Orexin-Producing Neurons: Interface of Systems of Emotion,
480 Energy Homeostasis and Arousal. *Trends Pharmacol. Sci.* **2011**, *32* (8), 451–462.
481 (20) Ito, N.; Yabe, T.; Gamo, Y.; Nagai, T.; Oikawa, T.; Yamada, H.; Hanawa, T. I.c.v. Administration of
482 Orexin-A Induces an Antidepressive-like Effect through Hippocampal Cell Proliferation.
483 *Neuroscience* **2008**, *157* (4), 720–732.
484 (21) Johnson, P. L.; Truitt, W.; Fitz, S. D.; Minick, P. E.; Dietrich, A.; Sanghani, S.; Träskman-Bendz, L.;
485 Goddard, A. W.; Brundin, L.; Shekhar, A. A Key Role for Orexin in Panic Anxiety. *Nat. Med.* **2010**,
486 *16* (1), 111–115.
487 (22) Johnson, P. L.; Molosh, A.; Fitz, S. D.; Truitt, W. A.; Shekhar, A. Orexin, Stress, and Anxiety/Panic
488 States. *Prog. Brain Res.* **2012**, *198*, 133–161.

489 (23) Deats, S. P.; Adidharma, W.; Lonstein, J. S.; Yan, L. Attenuated Orexinergic Signaling Underlies
490 Depression-like Responses Induced by Daytime Light Deficiency. *Neuroscience* **2014**, *272*, 252–260.
491 (24) Date, Y.; Ueta, Y.; Yamashita, H.; Yamaguchi, H.; Matsukura, S.; Kangawa, K.; Sakurai, T.;
492 Yanagisawa, M.; Nakazato, M. Orexins, Orexigenic Hypothalamic Peptides, Interact with Autonomic,
493 Neuroendocrine and Neuroregulatory Systems. *Proc. Natl. Acad. Sci. U. S. A.* **1999**, *96* (2), 748–753.
494 (25) Kuwaki, T. Orexin Links Emotional Stress to Autonomic Functions. *Auton. Neurosci.* **2011**, *161* (1–
495 2), 20–27.
496 (26) Nagahara, T.; Saitoh, T.; Kutsumura, N.; Irukayama-Tomobe, Y.; Ogawa, Y.; Kuroda, D.; Gouda, H.;
497 Kumagai, H.; Fujii, H.; Yanagisawa, M.; Nagase, H. Design and Synthesis of Non-Peptide, Selective
498 Orexin Receptor 2 Agonists. *J. Med. Chem.* **2015**, *58* (20), 7931–7937.
499 (27) Irukayama-Tomobe, Y.; Ogawa, Y.; Tominaga, H.; Ishikawa, Y.; Hosokawa, N.; Ambai, S.; Kawabe,
500 Y.; Uchida, S.; Nakajima, R.; Saitoh, T.; Kanda, T.; Vogt, K.; Sakurai, T.; Nagase, H.; Yanagisawa,
501 M. Nonpeptide Orexin Type-2 Receptor Agonist Ameliorates Narcolepsy-Cataplexy Symptoms in
502 Mouse Models. *Proc. Natl. Acad. Sci. U. S. A.* **2017**, *114* (22), 5731–5736.
503 (28) Hong, C.; Byrne, N. J.; Zamlynny, B.; Tummala, S.; Xiao, L.; Shipman, J. M.; Partridge, A. T.;
504 Minnick, C.; Breslin, M. J.; Rudd, M. T.; Stachel, S. J.; Rada, V. L.; Kern, J. C.; Armacost, K. A.;
505 Hollingsworth, S. A.; O'Brien, J. A.; Hall, D. L.; McDonald, T. P.; Strickland, C.; Brooun, A.; Soisson,
506 S. M.; Hollenstein, K. Structures of Active-State Orexin Receptor 2 Rationalize Peptide and Small-
507 Molecule Agonist Recognition and Receptor Activation. *Nat. Commun.* **2021**, *12* (1), 815.
508 (29) Fujimoto, T.; Rikimaru, K.; Fukuda, K.; Sugimoto, H.; Masuda, K.; Ohyabu, N.; Banno, Y.; Tokunaga,
509 N.; Kawamoto, T.; Tomata, Y.; Kumagai, Y.; Iida, M.; Nagano, Y.; Yoneyama-Hirozane, M.; Shimizu,
510 Y.; Sasa, K.; Ishikawa, T.; Yukitake, H.; Ito, M.; Aoyama, K.; Matsumoto, T. Discovery of TAK-925
511 as a Potent, Selective, and Brain-Penetrant Orexin 2 Receptor Agonist. *ACS Med. Chem. Lett.* **2022**,
512 *13* (3), 457–462.
513 (30) Yukitake, H.; Fujimoto, T.; Ishikawa, T.; Suzuki, A.; Shimizu, Y.; Rikimaru, K.; Ito, M.; Suzuki, M.;
514 Kimura, H. TAK-925, an Orexin 2 Receptor-Selective Agonist, Shows Robust Wake-Promoting
515 Effects in Mice. *Pharmacol. Biochem. Behav.* **2019**, *187*, 172794.

516 (31) Zhang, D.; Perrey, D. A.; Decker, A. M.; Langston, T. L.; Mavanji, V.; Harris, D. L.; Kotz, C. M.;
517 Zhang, Y. Discovery of Arylsulfonamides as Dual Orexin Receptor Agonists. *J. Med. Chem.* **2021**, *64*
518 (12), 8806–8825.
519 (32) Hino, T.; Saitoh, T.; Nagumo, Y.; Yamamoto, N.; Kutsumura, N.; Irukayama-Tomobe, Y.; Ishikawa,
520 Y.; Tanimura, R.; Yanagisawa, M.; Nagase, H. Design and Synthesis of Novel Orexin 2 Receptor
521 Agonists Based on Naphthalene Skeleton. *Bioorg. Med. Chem. Lett.* **2022**, *59*, 128530.
522 (33) Iio, K.; Saitoh, T.; Ohshita, R.; Hino, T.; Amezawa, M.; Takayama, Y.; Nagumo, Y.; Yamamoto, N.;
523 Kutsumura, N.; Irukayama-Tomobe, Y.; Ishikawa, Y.; Tanimura, R.; Yanagisawa, M.; Nagase, H.
524 Discovery of Orexin 2 Receptor Selective and Dual Orexin Receptor Agonists Based on the Tetralin
525 Structure: Switching of Receptor Selectivity by Chirality on the Tetralin Ring. *Bioorg. Med. Chem.*
526 *Lett.* **2022**, *60*, 128555.
527 (34) Konishi, H.; Sekino, T.; Manabe, K. Palladium-Catalyzed External-CO-Free Carbonylation of Aryl
528 Bromides Using 2,4,6-Trichlorophenyl Formate. *Chem. Pharm. Bull.* **2018**, *562* (5), 562–567.
529 (35) Narita, M.; Nagumo, Y.; Miyatake, M.; Ikegami, D.; Kurahashi, K.; Suzuki, T. Implication of Protein
530 Kinase C in the Orexin-Induced Elevation of Extracellular Dopamine Levels and Its Rewarding Effect.
531 *Eur. J. Neurosci.* **2007**, *25* (5), 1537–1545.
532 (36) Jeong, Y.; Holden, J. E. The Role of Spinal Orexin-1 Receptors in Posterior Hypothalamic Modulation
533 of Neuropathic Pain. *Neuroscience* **2009**, *159* (4), 1414–1421.
534 (37) Chiou, L.-C.; Lee, H.-J.; Ho, Y.-C.; Chen, S.-P.; Liao, Y.-Y.; Ma, C.-H.; Fan, P.-C.; Fuh, J.-L.; Wang,
535 S.-J. Orexins/Hypocretins: Pain Regulation and Cellular Actions. *Curr. Pharm. Des.* **2010**, *16* (28),
536 3089–3100.
537 (38) Inutsuka, A.; Yamashita, A.; Chowdhury, S.; Nakai, J.; Ohkura, M.; Taguchi, T.; Yamanaka, A. The
538 Integrative Role of Orexin/Hypocretin Neurons in Nociceptive Perception and Analgesic Regulation.
539 *Sci. Rep.* **2016**, *6*, 29480.
540 (39) Suzuki, T.; Masukawa, Y.; Misawa, M. Drug Interactions in the Reinforcing Effects of Over-the-
541 Counter Cough Syrups. *Psychopharmacology* **1990**, *102* (4), 438–442.

(40) Ohsawa, M.; Kamei, J. Modification of Kappa-Opioid Receptor Agonist-Induced Antinociception by Diabetes in the Mouse Brain and Spinal Cord. *J Pharmacol Sci.* **2005**, 98(1), 25–32.

(41) Khroyan, TV.; Cippitelli, A.; Toll, N.; Lawson, JA.; Crossman, W.; Polgar, WE.; Toll, L. *In Vitro* and *In Vivo* Profile of PPL-101 and PPL-103: Mixed Opioid Partial Agonist Analgesics with Low Abuse Potential. *Front Psychiatry*. **2017**, 8, 52.

Table of Contents Graphic